ARTICLE

Investigation of Ultrafast Photoisomerization Dynamics of Azobenzene Derivative (*E*)-1-Phenyl-2-((triisopropylsilyl)ethynyl)diazene†

Yilan Lin[a‡], Xiaofan Wei[a‡], Dong Fang[b], Ziyu Wang[a], Yifan Huang[a], Tao Li[b], Weimin Liu[a*]

a. School of Physical Science and Technology, ShanghaiTech University, Shanghai 201210, China
b. School of Chemistry and Chemical Engineering, Frontiers Science Center for Transformative Molecules, Shanghai Key Laboratory of Electrical Insulation and Thermal Aging, Shanghai Jiao Tong University, Shanghai 200240, China

(Dated: Received on December 1, 2023; Accepted on December 19, 2023)

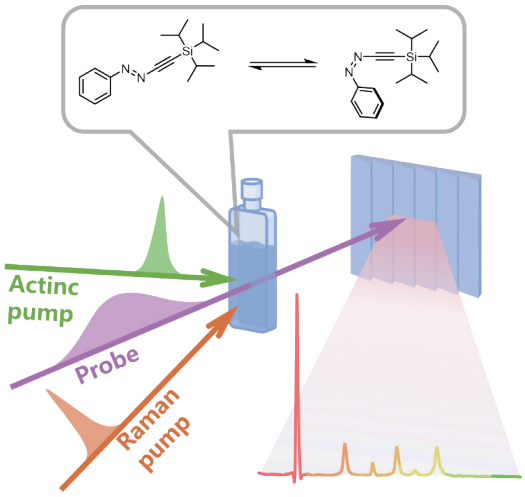

When exposed to light at a specific wavelength, azobenzene and its derivatives experience a transformation from *trans* form to *cis* form through isomerization. Due to its ability to change color upon illumination, azobenzene finds extensive use in various molecular devices and functional materials. However, despite significant researches focused on practical applications, there are still ongoing investigations into the underlying mechanisms governing azobenzene's photochemical reactions and isomerization. In this study, we employ femtosecond stimulated Raman spectroscopy (FSRS), and transient absorption spectroscopy, in conjunction with quantum chemical calculations, to elucidate the ultrafast isomerization dynamics of an azobenzene derivative known as *trans*-AZOTIPS ((*E*)-1-phenyl-2-((triisopropylsilyl)ethynyl)diazene). The results demonstrate that upon photoexcitation, rapid isomerization occurs along the C–N=N bonds via the singlet excited state S_1 to hot ground state (S_0^*) state transition. Additionally, we explore the impact of solvent viscosity on the isomerization process and find that the duration of isomerization remains unaffected by variations in solvent viscosity. These results suggest that the isomerization pathway involves a volume-conserving motion known as "hula twist". After that, the vibrational cooling process is obtained in S_0 state.

Key words: Azobenzene derivative, Isomerization, Femtosecond stimultated Raman spectroscopy, Hula twist

I. INTRODUCTION

The photo-isomerism, accessibility, and tunability of azobenzene make it a widely employed photoswitching molecule. Among these properties, photo-isomerization is the fundamental characteristic of an optical switch [1]. These molecules exhibit *cis-trans* conformations and undergo structural changes between the two conformations when excited by light, thereby achieving the function of optical switching [2]. The photoinduced isomerization dynamics has been extensively investigated using various ultrafast spectroscopic techniques, includ-

† Part of Special Topic "Ultrafast Spectroscopy focused on Ultrafast Dynamics and Molecular Structures".
‡ These authors contributed equally to this work.
* Author to whom correspondence should be addressed. E-mail: liuwm@shanghaitech.edu.cn

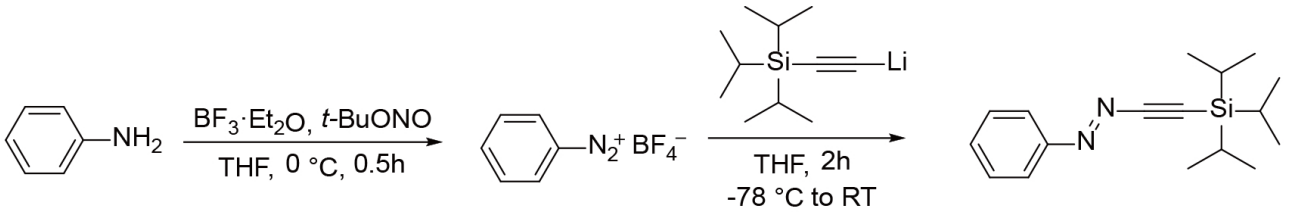

FIG. 1 Synthetic route of (*E*)-1-phenyl-2-((triisopropylsilyl)ethynyl)diazene molecule.

ing transient absorption [3–5], femtosecond fluorescence upconversion [6], and femtosecond Raman spectroscopy [7, 8]. Despite extensive researches on excited-state structural dynamics processes in azobenzene and its derivatives, the mechanism of isomerization in azobenzene molecules remains a topic of ongoing debate. The proposed isomerization pathway involves three distinct processes: torsion around the central N=N double bond [6, 9–11], inversion of the nitrogen center when the phenyl rings align in the molecular plane [2, 11–14], and a multidimensional phenomenon which is known as hula twist. This hula twist exhibits coordinated movement resembling that of a pedal, involving both nitrogens and phenyls [8].

The present study involves the synthesis of a novel *trans*-azobenzene derivative, namely (*E*)-1-phenyl-2-((triisopropylsilyl)ethynyl)diazene, abbreviated as *trans*-AZOTIPS (see FIG. 1). This synthetic process entails substituting the aryl ring with a non-aryl group on one side of the original azobenzene's phenyl ring. The substitution occurs at the N=N double bond connecting it to the benzene ring and further extends to the acetylene moiety, ultimately terminating at the triisopropylsilyl (TIPS) silicon group. The shape of one side of the N=N changes from a "ring" to a "line", and this structural difference may significantly impact the molecule's fundamental optical properties. In comparison with other aliphatic aryl azobenzene compounds that substitute aryl rings with non-aryl groups, *trans*-AZOTIPS demonstrates enhanced stability and offers potential for tailored modifications in its optical switching properties through variations in the ethyl group within its silicon linkage [15].

We strategically combined tunable femtosecond stimulated Raman spectroscopy (FSRS) and transient absorption (TA) to elucidate the photoisomerization events of the *trans*-AZOTIPS molecule. The detailed reaction pathways for *trans*-AZOTIPS photoisomerization were dissected, revealing an initial volume-conserving "hula twist" along the C–N=N bonds via the S_1 to hot S_0^* state transition, followed by a process of S_0 state vibrational cooling.

II. MATERIALS AND METHODS

To a stirred solution of aniline (0.46 g, 5 mmol, 1.0 eq.) in THF (10.0 mL) was added $BF_3{\cdot}Et_2O$ (0.9 g, 6 mmol, 1.2 eq.) dropwise. Then, the mixture was added *tert*-butyl nitrite (*t*-BuONO) (0.6 g, 6 mmol, 1.2 eq.) slowly at 0 °C for 30 min. The precipitate was filtered off, washed with excess Et_2O, and dried in a vacuum to obtain PhN_2BF_4. The product was used without further purification.

To an ice-cooled solution of triisopropylsilylacetylene (0.9 g, 5 mmol, 1.0 eq.) in dry THF (10 mL) under Ar atmosphere was slowly added *n*-BuLi in hexane (3.1 mL, ca. 1.6 mol/L, 6 mmol, 1.1 eq.). After 30 min, the solution was then quickly transferred to a suspension of PhN_2BF_4 (1.15 g, 6 mmol, 1.0 eq.) in dry THF (15 mL) at −78 °C under Ar. The reaction mixture was then warmed to room temperature over 1 h. Subsequently, the reaction was quenched by adding saturated aqueous $NaHCO_3$ (10 mL) and was extracted with EtOAc (10 mL × 3). The combined organic layer was washed with brine (20 mL), dried over $MgSO_4$, and concentrated under reduced pressure. The residue was purified by flash column chromatography to afford (*E*)-1-phenyl-2-((triisopropylsilyl)ethynyl)diazene (red oil, 1.17 g, 82% yield).

In the femtosecond stimulated Raman spectroscopy (FSRS), the fundamental laser pulses (Astrella USP, Coherent, Inc.) with 800 nm center wavelength, 35 fs pulse duration, 7 mJ pulse energy, and 1 kHz repetition rate were split into three beams to generate a tunable narrowband picosecond (ps) Raman pump, a broadband femtosecond (fs) Raman probe, and an fs actinic pump. The actinic pump centered at 330 nm was generated by an optical parametric amplifier (OPerA Solo, Coherent, Inc.) for excited-state FSRS. About 3 W of fundamental pulses was directed through a second harmonic bandwidth compressor (SHBC, Coherent, Inc.) to produce ps 400 nm Raman pump pulses. About

DOI: 10.1063/1674-0068/cjcp2312119

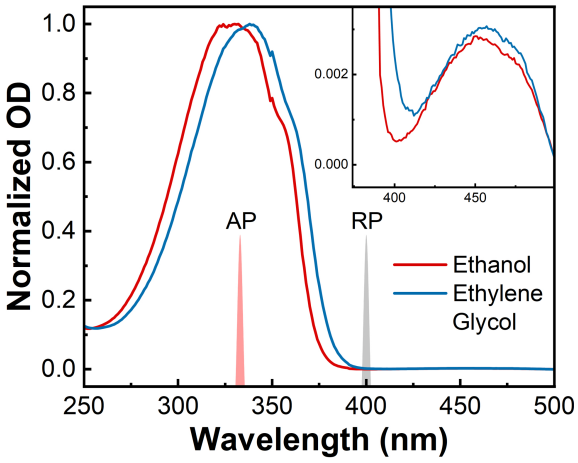

FIG. 2 The normalized steady-state absorption of *trans*-AZOTIPS in ethanol and ethylene glycol. The actinic pump (AP) and Raman pump (RP) wavelengths in FSRS experiments are shown as colored spikes.

15 mW of the fundamental laser output was focused onto a 2-mm-sapphire plate to obtain the supercontinuum white light as a Raman probe. The instrument response time was measured to be ~150 fs by cross correlation between the fs actinic pump and Raman probe pulses.

The geometries of (*E*)-1-phenyl-2-((triisopropylsilyl)-ethynyl) diazene with a *cis*- and *trans*-configurations at ground state were fully optimized. The vibrational spectra were simulated by using the optimized geometries. The geometric optimization and vibrational spetra simulation were carried out by using the functional of PBE0. The basis set of 6-311+G** was employed to describ all the elements of (*E*)-1-phenyl-2-((triisopropylsilyl)ethynyl)diazene. The solvation effect was included by using the polarizable continuum model. These computations were performed by using the software package of Gaussian 09 (RevE.01).

III. RESULTS AND DISCUSSION

The steady-state absorption spectra of *trans*-AZOTIPS in ethanol (polarity: 4.3; coefficient of viscosity: 1.1 mPa·s) and ethylene glycol (polarity: 6.9; coefficient of viscosity: 19.9 mPa·s) are depicted in FIG. 2. In ethanol, *trans*-AZOTIPS exhibits a prominent absorption peak centered at 330 nm, which undergoes a redshift to 340 nm upon solvent change to ethylene glycol. The observed redshift of the absorption band can be attributed to the influence of the solvent polarity. Additionally, both *trans*-AZOTIPS in ethanol and ethylene glycol display a minute shoulder around 450 nm. The absorption peak at around 330 nm is ascribed to the absorption of ππ* (S_2←S_0) band, while the weak peak at 450 nm corresponds to the nπ* (S_1←S_0) band absorption of *trans*-AZOTIPS [16–18].

We first used femtosecond transient absorption (TA) spectroscopy to investigate the kinetic of *trans*-AZOTIPS upon photoexcitation of ππ* (S_2) band using 330 nm photoexcitation, and FIG. 3(a, b) shows the TA spectra of *trans*-AZOTIPS dissolved in ethanol and ethylene glycol within a 45 ps detection time window. The two-dimensional (2D) TA spectra of both samples exhibit intricate excited-state features in the probe wavelength range spanning from 350 nm to 620 nm, encompassing a ground state bleaching (GSB) band at the blue edge of the TA spectra, an excited-state absorption (ESA) band ranging from 360 nm to 400 nm, and an ESA band on the red side of the TA spectra, displaying ultrafast decay dynamics. A global fit based on the evolution-associated difference spectra (EADS) is shown at the bottom of FIG. 3(a, b). The TA spectra in ethanol are fitted satisfactorily with a model consisting of two exponential decay components, including τ_1 = 170 fs, τ_2=4 ps. Notably, unlike the *trans*-AZOTIPS, as shown in FIG. 3(c), the EADS spectra of *trans*-azobenzene reveal three exponential decay components including τ_1=100 fs, τ_2=690 fs, and τ_3=7.4 ps. The previous ultrafast spectroscopies suggest that, upon the ππ* (S_2←S_0) excitation of *trans*-azobenzene, the relaxation processes occur from excited states S_2 to S_1 (τ_1=100 fs) and from excited state S_1 to hot ground state S_0^* (τ_2=690 fs), following vibrational cooling of S_0 state (τ_3=7.4 ps) [5, 8, 13, 14, 18–20].

For *trans*-AZOTIPS in ethanol (shown in FIG. 3(a)), the two decay components in EADS spectra can be attributed to the relaxation dynamics of S_1 to S_0^* (τ_1=170 fs) and vibrational cooling dynamics of the S_0 state (τ_2=4 ps). The decay dynamics of S_2 to S_1 state cannot be observed, likely due to its lifetime being shorter than the instrument response function of TA (~120 fs). To further confirm this hypothesis, we employed a 450 nm actinic pump for exciting the S_1 (nπ*) state of *trans*-AZOTIPS in ethanol. FIG. 4 illustrates a comparison of TA spectra obtained by photoexcitation via ππ* and nπ* bands, probing at 400 nm. Both kinetics showcase identical two-exponential decay processes. Furthermore, the initial oscillation feature observed in TA dynamics upon excitation of both ππ* and nπ* bands is attributed to the coherent artificial effect induced by ethanol solvents. To probe the possible pho-

DOI: 10.1063/1674-0068/cjcp2312119

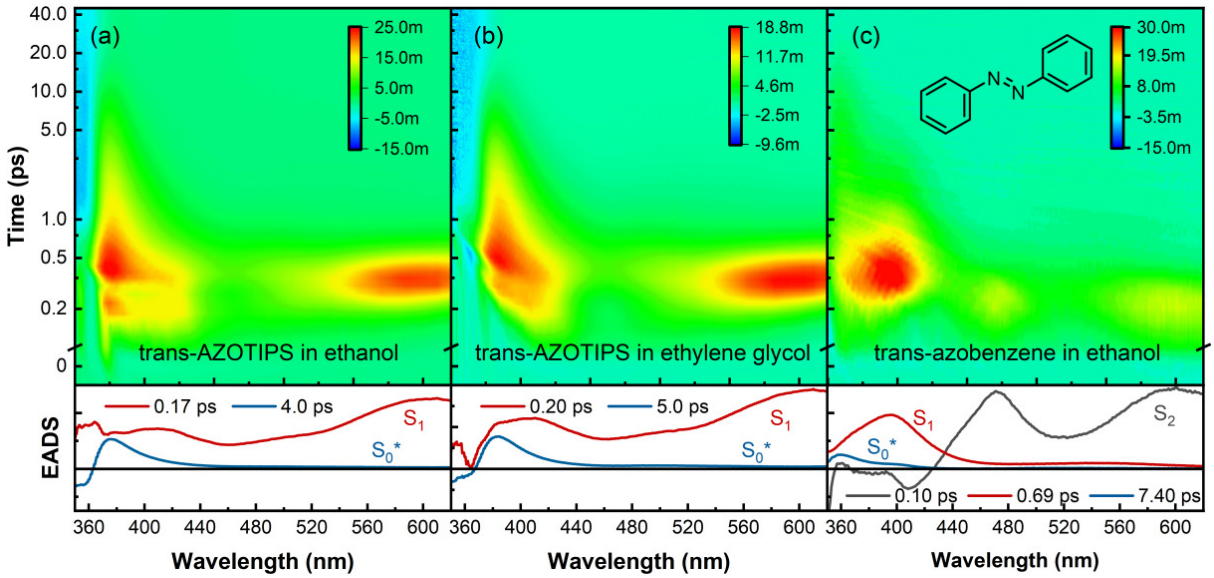

FIG. 3 The two-dimensional TA spectra (upper panel) and evolution-associated difference spectra (EADS, lower panel) global fit of *trans*-AZOTIPS in (a) ethanol, and (b) ethylene glycol. (c) The two-dimensional TA spectra and EADS global fit of *trans*-azobenzene in ethanol.

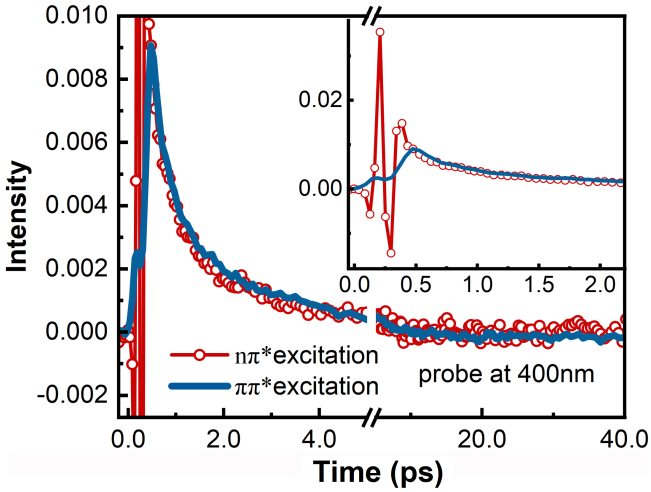

FIG. 4 Kinetics of *trans*-AZOTIPS in ethanol probe at 400 nm with nπ* (red dot line) and ππ* excitation (solid blue line). The enlarged plot with coherent artificial effect decay up to 2 ps is shown in the inset.

toisomerization of *trans*-AZOTIPS during the primary photo-processes, the *trans*-AZOTIPS sample was examined in high-viscosity ethylene glycol. As shown in FIG. 3(b), the lifetimes estimated using EADS for the two exponential components are 200 fs (τ_1), and 5 ps (τ_2). Notably, the spectral shape of the global analysis of each component does not differ from that obtained in the ethanol solvent, indicating that the intermediate states of the *trans*-AZOTIPS remain unchanged in the high-viscosity solvent.

Theoretical calculations and experimental results for *trans*-azobenzene suggest that the relaxation process of $S_1 \rightarrow S_0$ is primarily governed by isomerization [2, 8, 18, 21]. However, in our experiment the first decay component τ_1 in *trans*-AZOTIPS remains unaffected by changes in solvent viscosity. Does that mean that no isomerization occurs during the $S_1 \rightarrow S_0$ transition in *trans*-AZOTIPS?

To address this question and gain insights into the structural dynamics beyond electronic features, femtosecond stimulated Raman spectroscopy (FSRS) was employed to monitor the vibrational marker bands associated with excited states of *trans*-AZOTIPS. FIG. 5 (a, b) shows the time-resolved FSRS spectra of *trans*-AZOTIPS in ethanol and ethylene glycol across a frequency range of 1100–1600 cm^{-1}. We strategically selected a 400 nm Raman pump near the peak of the *trans*-AZOTIPS ESA band to provide resonantly enhanced excited-state Raman signals, which comprise decay and rise dynamics that track the photoinduced structural dynamics of the *trans*-AZOTIPS. Based on the TA experimental results, the observed transient dynamics in FSRS can be attributed to the sequential transition of $S_1 \rightarrow S_0^* \rightarrow S_0$. In ethanol, *trans*-AZOTIPS exhibits the emergence of a broad Raman band at 1370 cm^{-1}, which subsequently undergoes ultrafast decays. Following this, a new Raman mode emerges at 1357 cm^{-1} and then experiences a decay in intensity within 10 ps. When *trans*-AZOTIPS is dissolved in ethylene glycol, the Raman modes shift to 1375 cm^{-1} and 1356 cm^{-1}.

Based on a density functional theory (DFT) calcula-

DOI: 10.1063/1674-0068/cjcp2312119

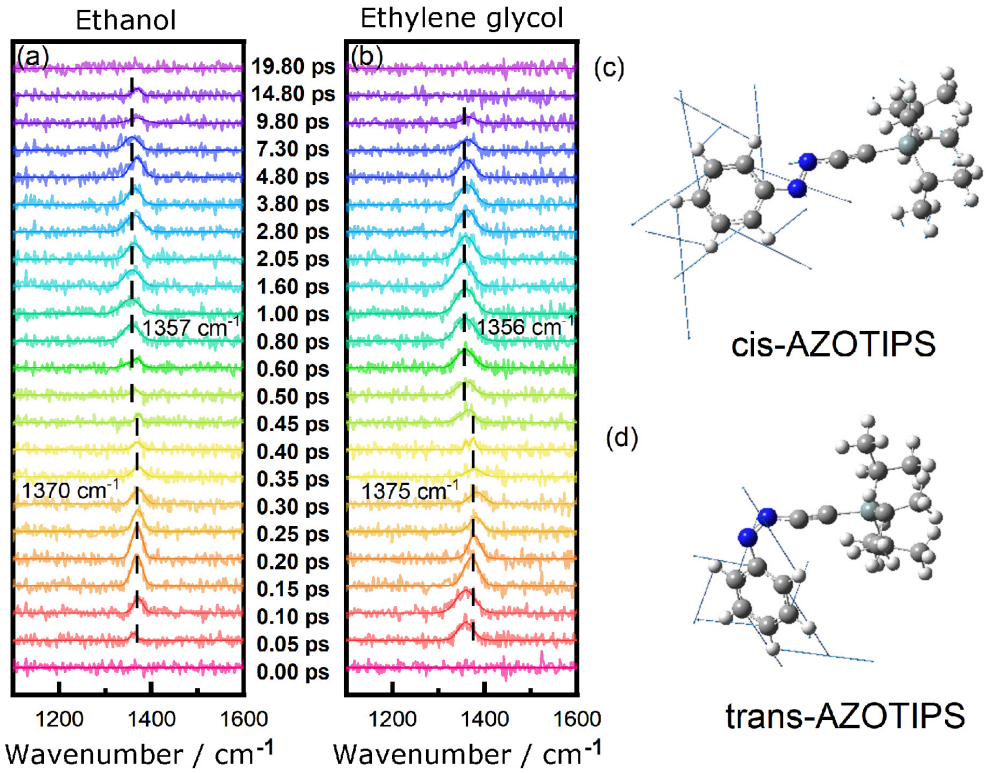

FIG. 5 FSRS spectra of *trans*-AZOTIPS under 330 nm excitation in (a) ethanol and (b) ethylene glycol in the frequency range of 1100–1600 cm^{-1} (the delay time points are indicated between (a) and (b)). DFT calculation shows the optimized structure and Raman model of (c) *cis*-AZOTIPS and (d) *trans*-AZOTIPS.

tion for *trans*-AZOTIPS in ethanol (see FIG. 5(c, d)), the observed excited state Raman modes at 1370 cm^{-1} (1375 cm^{-1}) are mainly attributed to the C–H in-plane bending and ring stretching of the phenyl ring combined with the bending motion of C–N=N. This motion in *trans*-AZOTIPS implies isomerization through the C–N=N bands. Additionally, as depicted in FIG. 6(a), the transient amplitude of this Raman mode is independent of viscosity and exhibits a single exponential decay with a time constant of approximately 100 fs in both solvents. This behavior suggests a conformational change occurring via $S_1 \rightarrow S_0^*$ transition within a specific confined volume associated with the C–N=N bands. Previous studies have revealed a rotational isomerization motion known as hula twist (HT) in *trans*-azobenzene [8, 22, 23]. The HT motion has been reported for previtamin D [24], bilirubin [25], the confined visual chromophore in rhodopsin [26], and fluorescent protein [27, 28]. Importantly, in contrast to the proposed torsional or inversion motion of the *trans*-azobenzene molecule [2, 6, 9–14], this HT process in *trans*-AZOTIPS involves the pedal-like rotation of C–N=N bonds, resulting in the convergence of phenyl groups within the molecular plane. Consequently, this mechanism remains unaffected by viscosity effects present in the surrounding medium [8].

As a result, the isomerization occurring in S_1 state leads to the formation of *cis*-AZOTIPS in hot ground state S_0^*. Based on DFT calculations, as shown in FIG. 5(d), the subsequent Raman mode at 1357 cm^{-1} (1356 cm^{-1}) is assigned to the C–H in-plane bending and ring stretching of phenyl ring combined with the bending motion of C–N=N for *cis*-AZOTIPS. As illustrated in FIG. 6(b), the relaxation of the S_0^* state on a picosecond timescale can be attributed to vibrational cooling of the hot ground state [29]. Furthermore, the Raman mode exhibits a significant blue shift (see FIG. 6(c, d)) within several ps supporting a well-defined vibrational cooling process [29]. Notably, the vibrational cooling dynamics in high viscous ethylene glycol solvent exhibit a shorter decay lifetime (5.8 ps) than that in ethanol (7.8 ps) which is consistent with previous studies on *trans*-stilbene, indicating higher viscosity coefficients lead to faster cooling time [30].

IV. CONCLUSION

In this study, we employ FSRS and TA experiments

DOI: 10.1063/1674-0068/cjcp2312119

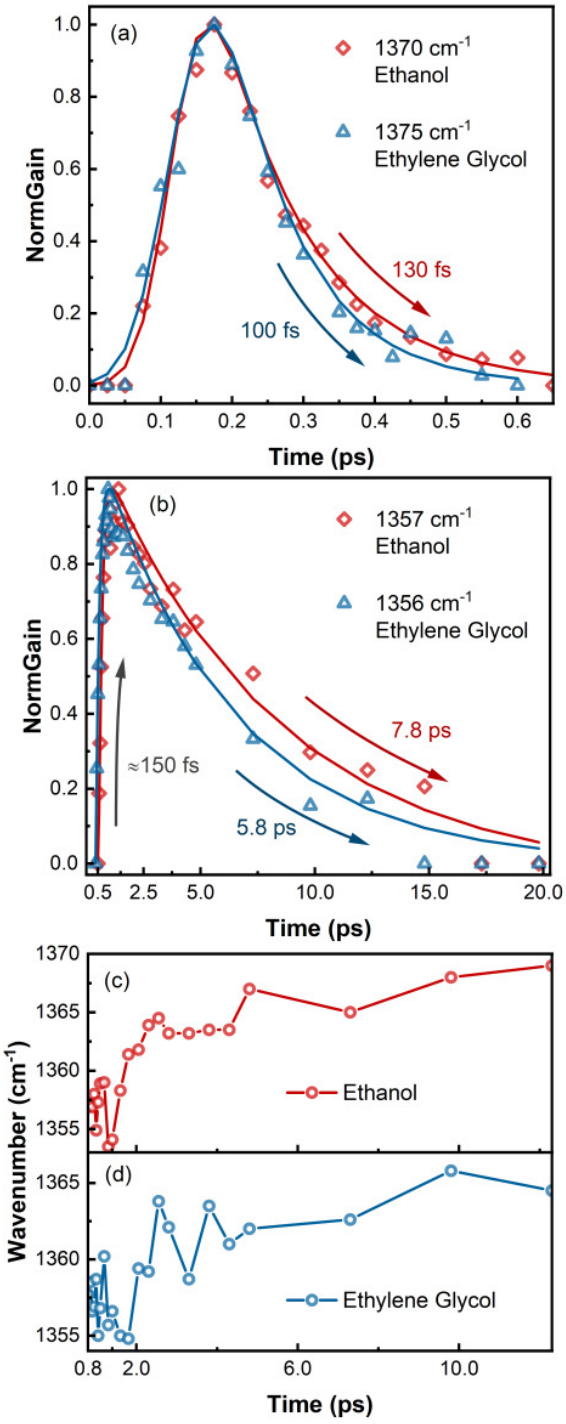

FIG. 6 (a) Transient amplitude of the Raman mode at 1370 cm^{-1} (ethanol) and 1375 cm^{-1} (ethylene glycol); (b) transient amplitude of the Raman mode at 1357 cm^{-1} (ethanol) and 1356 cm^{-1} (ethylene glycol); transient frequency shift of the mode at (c) 1357 cm^{-1} (ethanol) and (d) 1356 cm^{-1} (ethylene glycol).

assisted by DFT calculations to elucidate the excited-state structural dynamics of *trans*-AZOTIPS in various solvents. Based on the experimental findings, we can summarize the dynamics of configurational isomerization processes observed in *trans*-AZOTIPS photoreaction (see FIG. 7). Upon excitation of *trans*-AZOTIPS to the ππ* (S_2) state, it rapidly undergoes internal conversion from S_2 to S_1 state within a few tens of femtoseconds. Subsequently, the detection of C–H in-plane bending and phenyl ring stretching combined with the bending motion of C–N=N bonds signifies the prompt decay of *trans*-AZOTIPS signals from S_1 to S_0^* state through *trans*-to-*cis* isomerization. Furthermore, this Raman mode exhibits insensitivity towards solvent viscosity, suggesting that volume-conserving HT mechanisms dominate the configurational isomerization process from $S_1 \rightarrow S_0^*$ state. Finally, the population in the S_0^* state relaxes to ground-state *cis*-AZOTIPS (S_0) within several picoseconds.

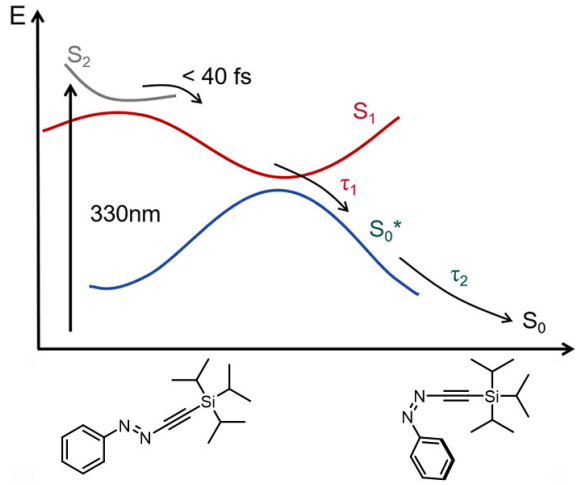

FIG. 7 A scheme of excited state deactivation model of *trans*-AZOTIPS at ππ* excitation.

[1] G. S. Hartley, Nature **140**, 281 (1937).
[2] H. Rau and E. Lueddecke, J. Am. Chem. Soc. **104**, 1616 (1982).
[3] H. Satzger, S. Spörlein, C. Root, J. Wachtveitl, W. Zinth, and P. Gilch, Chem. Phys. Lett. **372**, 216 (2003).
[4] H. Satzger, C. Root, and M. Braun, J. Phys. Chem. A **108**, 6265 (2004).
[5] C. J. Otolski, A. M. Raj, V. Ramamurthy, and C. G. Elles, Chem. Sci. **11**, 9513 (2020).
[6] Y. C. Lu, C. W. Chang, and E. W. G. Diau, J. Chin. Chem. Soc. **49**, 693 (2002).
[7] A. L. Dobryakov, M. Quick, I. Ioffe, A. A. Granovsky, N. P. Ernsting, and S. A. Kovalenko, J. Chem. Phys. **140**, 184310 (2014).
[8] M. Quick, A. L. Dobryakov, M. Gerecke, C. Richter,

DOI: 10.1063/1674-0068/cjcp2312119

F. Berndt, I. N. Ioffe, A. A. Granovsky, R. Mahrwald, N. P. Ernsting, and S. A. Kovalenko, J. Phys. Chem. B **118**, 8756 (2014).
[9] J. L. Magee, W. Shand Jr., and H. Eyring, J. Am. Chem. Soc. **63**, 677 (1941).
[10] I. K. Barker, V. Fawcett, and D. A. Long, J. Raman Spectrosc. **18**, 71 (1987).
[11] C. M. Stuart, R. R. Frontiera, and R. A. Mathies, J. Phys. Chem. A **111**, 12072 (2007).
[12] H. Rau and Y. Q. Shen, J. Photochem. Photobiol. A: Chem. **42**, 321 (1988).
[13] T. Fujino and T. Tahara, J. Phys. Chem. A **104**, 4203 (2000).
[14] T. Fujino, S. Y. Arzhantsev, and T. Tahara, J. Phys. Chem. A **105**, 8123 (2001).
[15] Y. Zhang, C. C. Huang, X. R. Lin, Q. Hu, B. Y. Hu, Y. L. Zhou, and G. G. Zhu, Org. Lett. **21**, 2261 (2019).
[16] C. L. Forber, E. C. Kelusky, N. J. Bunce, and M. C. Zerner, J. Am. Chem. Soc. **107**, 5884 (1985).
[17] T. Cusati, G. Granucci, M. Persico, and G. Spighi, J. Chem. Phys. **128**, 194312 (2008).
[18] H. M. D. Bandara and S. C. Burdette, Chem. Soc. Rev. **41**, 1809 (2012).
[19] I. K. Lednev, T. Q. Ye, R. E. Hester, and J. N. Moore, J. Phys. Chem. **100**, 13338 (1996).
[20] I. K. Lednev, T. Q. Ye, P. Matousek, M. Towrie, P. Foggi, F. V. R. Neuwahl, S. Umapathy, R. E. Hester, and J. N. Moore, Chem. Phys. Lett. **290**, 68 (1998).
[21] C. R. Crecca and A. E. Roitberg, J. Phys. Chem. A **110**, 8188 (2006).
[22] M. Bo̎ckmann, N. L. Doltsinis, and D. Marx, J. Phys. Chem. A **114**, 745 (2010).
[23] M. Böckmann, N. L. Doltsinis, and D. Marx, J. Chem. Phys. **137**, 22A505 (2012).
[24] A. M. Müller, S. Lochbrunner, W. E. Schmid, and W. Fuß, Angew. Chem. Int. Ed. **37**, 505 (1998).
[25] R. H. Pu, Z. Y. Wang, R. X. Zhu, J. M. Jiang, T. C. Weng, Y. F. Huang, and W. M. Liu, J. Phys. Chem. Lett. **14**, 809 (2023).
[26] R. S. H. Liu and G. S. Hammond, Photochem. Photobiol. Sci. **2**, 835 (2003).
[27] Q. Q. Zhang, X. B. Chen, G. L. Cui, W. H. Fang, and W. Thiel, Angew. Chem. **126**, 8793 (2014).
[28] Z. Y. Wang, Y. Zhang, C. Chen, R. X. Zhu, J. M. Jiang, T. C. Weng, Q. J. Ji, Y. F. Huang, C. Fang, and W. M. Liu, Angew. Chem. Int. Ed. **62**, e202212209 (2023).
[29] W. M. Liu, L. T. Tang, B. G. Oscar, Y. L. Wang, C. Chen, and C. Fang, J. Phys. Chem. Lett. **8**, 997 (2017).
[30] I. Koichi, Y. Kyousuke, T. Yuta, and H. Hiro-o, Chem. Lett. **36**, 504 (2007).

DOI: 10.1063/1674-0068/cjcp2312119